

Precision topography of a reversing sand dune at Bruneau Dunes, Idaho, as an analog for Transverse Aeolian Ridges on Mars



James R. Zimbelman*, Stephen P. Scheidt

Center for Earth and Planetary Studies, National Air and Space Museum, MRC 315, Smithsonian Institution, Washington, DC 20013-7012, USA

ARTICLE INFO

Article history:

Available online 13 August 2013

Keywords:

Mars, Surface
Mars
Earth
Geological processes
Data reduction techniques

ABSTRACT

Ten high precision topographic profiles across a reversing dune were created from a differential global position system (DGPS). The shapes of the profiles reveal a progression from immature to transitional to mature characteristics moving up the dune. When scaled by the basal width along each profile, shape characteristics can be compared for profiles whose horizontal scales differ by orders of magnitude. The comparison of width-scaled Bruneau Dunes profiles to similarly scaled profiles of Transverse Aeolian Ridges (TARs) on Mars indicates that many TARs are likely similar to transitional or mature reversing sand dunes.

Published by Elsevier Inc.

1. Introduction

A reversing sand dune is defined to be “a dune that tends to develop unusual height but migrates only a limited distance because seasonal shifts in direction of the dominant wind cause it to move alternately in nearly opposite directions” (Jackson, 1997, p. 545). The seasonal wind pattern is therefore bidirectional for reversing dunes, where the two dominant winds from nearly opposite directions are balanced with respect to strength and duration (McKee, 1979). The Bruneau Dunes in central Idaho are an excellent place to conduct a study of reversing sand dunes because here the dunes have grown to impressive heights in a wind regime that supports the development of reversing dunes rather than horizontally migrating dunes. The dunes are protected from off-road vehicular traffic because the main dune complex is located within the boundaries of the Bruneau Dunes State Park (Zimbelman and Williams, 2007). The Bruneau Dunes are a 1.5-h drive SE from Boise, and they are only 29 km (18 mi) south of the city of Mountain Home.

Recent data from Mars has stimulated interest in the collection of detailed topographic information about reversing dunes. The High Resolution Imaging Science Experiment (HiRISE) camera on the Mars Reconnaissance Orbiter spacecraft has returned over 20,000 images that reveal the martian surface in exquisite detail, with many of the images achieving a ground spatial resolution of 25 cm per pixel (McEwen et al., 2007). Early HiRISE images included some dramatic examples of aeolian bedforms that have

been given the non-genetic name ‘Transverse Aeolian Ridges’ (TARs), a general term proposed for linear to curvilinear aeolian features that could be the result of either dune or ripple formation processes (Bourke et al., 2003). Profiles derived from photogrammetry of TARs in HiRISE images showed that TARs larger than 1 m in height compared favorably to profiles of reversing dunes at Coral Pink Sand Dunes State Park in southern Utah, while TARs less than 0.5 m in height were very distinct from the reversing dune profiles but consistent with measured profiles of megaripples (Zimbelman, 2010).

In order to provide a test of the reversing dune hypothesis for large TARs on Mars, we collected a series of precision topographic profiles across one of the large reversing dunes at the Bruneau Dunes, as first reported at the Third Planetary Dunes workshop (Zimbelman and Scheidt, 2012). The resulting profiles provide valuable new information about probable stages of formation encountered during the growth of reversing dunes, as well as a possible tool for evaluating the relative state of evolution of reversing dunes. The profile series provides a template for evaluating the possible stages of evolution of individual TARs on Mars, under the working hypothesis that large TARs have profile shapes comparable to that of reversing dunes.

2. Background

The Bruneau Dunes State Park was formed in order to preserve a very unique natural area, as well as provide protection for the wildlife that make use of two lakes on the northwest side of the dunes (inset, Fig. 1). Established in 1970, the park covers 19.4 km² (4800 acres), including the tallest single-structured (i.e., not braced against other dunes or mountains) sand dune in North

* Corresponding author. Fax: +1 202 786 2566.

E-mail addresses: zimbelmanj@si.edu (J.R. Zimbelman), sscheidt77@gmail.com (S.P. Scheidt).

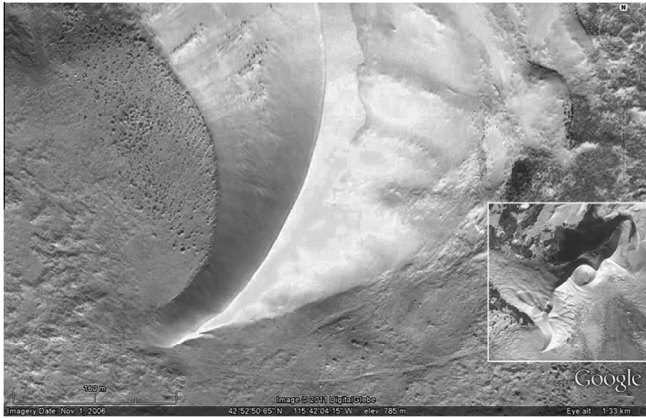


Fig. 1. Google Earth image mosaic of the study location at the southern end of the Bruneau Dunes, Idaho (11/1/06). North is to the top. Inset shows all of the largest dunes, and the lakes at their northern end.

America, which has 143 m (470 ft) of relief from the summit of the tallest dune to the lake level (for information about the park, see parksandrecreation.idaho.gov/parks/bruneau-dunes or www.idahoparks.org/state-parks/bruneau-dunes-state-park). The largest dunes are interpreted to be reversing dunes (Murphy, 1973), but features on the sides of the largest dunes suggest possible form flow interactions that can move sand in directions at large angles relative to the regional wind direction (Howard et al., 1978). There are some visual similarities between features observed on the Bruneau Dunes and patterns present on the arms of star dunes (e.g., Lancaster, 1989), where sand transport occurs oblique to crest orientation. The sheer size of the main Bruneau Dunes may induce complex local wind patterns on the sides of dunes.

The Bruneau Dunes are located approximately in the center of an old cut-off meander of the Snake River, now called Eagle Cove, that was carved into lacustrine sediments of the Glens Ferry and Bruneau Formations, which are from Upper Pliocene to Middle Pleistocene (respectively) in age (Murphy, 1973). The close proximity of Eagle Cove to the present day channel of the Snake River contributes significantly to a constraint for the probable initiation of the sand accumulation represented by the current large sand dunes.

The Snake River is the main drainage pathway for water to exit the southern portions of Idaho. This large river has carved a substantial canyon into the basalt lava flows that comprise the surface materials of the Snake River Plains, the largest physiographic province within southern Idaho. There is abundant geologic evidence that the present day Snake River is but a mere shadow of the major flood that passed through this river system during the Pleistocene (Malde, 1968). Glacial Lake Bonneville attained a level that overtopped its rim at Red Rock Pass in southeastern Idaho, leading to rapid downcutting at the site of the breach and the rapid release of 4700 km³ of water onto the Snake River Plains; erosional features and flood deposits along the Snake River Canyon indicate that the peak discharge during this catastrophic flood was most likely ~935,000 m³/s, so that a minimum duration of about 8 weeks was needed to move the total volume of released water through the canyon at the peak discharge rate (Jarrett and Malde, 1987; O'Connor, 1993). The massive Bonneville Flood occurred about 15,000 years ago (Jarrett and Malde, 1987), and it is presumed that the flood would have easily removed any aeolian sand deposits from Eagle Cove that pre-dated the flood (Murphy, 1973). The sand at the Bruneau Dunes consists (by volume) of 62% quartz, 26% feldspar, and 12% basaltic (iron-rich) particles, indicating a closer affinity to the nearby Bruneau and Glens Ferry Formation sediments than to the basalts and other rocks exposed upstream of Eagle Cove

(Murphy, 1973). Aeolian or fluvial activity would not have needed to transport the sand very far to get it into Eagle Cove. However, once sand got into Eagle Cove, the wind pattern is such that it likely could not have easily exited later.

Reversing sand dunes form under a bidirectional wind regime, where two dominant winds come from directions that are almost directly opposite of each other (McKee, 1979). The Remote Automated Weather Station (RAWS) system, operated by the U.S. government, has >1900 individual instrumented weather stations (as of 2002) spread throughout the conterminous United States, Alaska, and Hawaii (Zachariassen et al., 2003, p. 2). The Mountain Home Air Force Base (MHAFFB) RAWS station is located about 21 km NW of the Bruneau Dunes. Using a web-based access page, we obtained MHAFFB RAWS data from 2010, which clearly demonstrates a strong bimodal annual wind regime for the region, although minor winds can blow from a variety of directions during spring and fall (Fig. 2). It is justifiable to ask whether wind records obtained 21 km away from the study site reflect the wind conditions experienced at the dunes. We attempted to address this issue by installing an inexpensive weather-proof timelapse digital camera (known commercially as a 'GardenWatchCam') to obtain hourly images of the study site at the Bruneau Dunes. Use of timelapse digital cameras has proved to be a cost-effective method for monitoring sand mobility in previous aeolian studies (Lorenz, 2011; Lorenz and Valdez, 2011). During more than 2 years of GardenWatchCam monitoring of the study site (from April 27, 2011, through August 31, 2013), images of bidirectional intense saltation occurring at the south end of the dunes (Figs. 3 and 4) correlate very well with strong wind events (taken here to be >6 m/s average winds sustained for >3 h) recorded at the MHAFFB RAWS site, providing on-site validation that the bimodal wind pattern that dominates the RAWS data (Fig. 2) is consistent with the major sand-driving events observed to take place at the dunes.

In order to obtain precise topographic profiles of the sand dunes, we utilized a Differential Global Positioning System (DGPS). The equipment used in this project was a Trimble R8 Total Station, a carrier-phase DGPS system consisting of a stationary base receiver and a roving receiver to collect the individual survey points; this system provides horizontal accuracy of 1–2 cm and vertical accuracy of 2–4 cm, relative to the base station location (Zimbelman and Johnston, 2001). When combined with field notes and photographs tied to survey point locations, DGPS topographic data have proved to be very useful in addressing diverse geomorphic topics (e.g., Zimbelman and Johnston, 2001; Irwin and Zimbelman, 2012; Zimbelman et al., 2012). Precise topographic profiles across aeolian depositional features at diverse scales has proved to be very helpful in distinguishing between alternative formation mechanisms that have acted to generate the features (Zimbelman et al., 2012).

Topographic information for TARs on Mars have recently been derived from HiRISE image data (Zimbelman, 2010; Shockey and Zimbelman, 2013), generating profiles that can be compared to the measured profiles of aeolian features on Earth (Zimbelman et al., 2012). The study project at the Bruneau Dunes was carried out specifically in order to obtain a well constrained topographic data set for a reversing sand dune, to serve as a guide for evaluating the hypothesis that TARs > 1 m in height are most similar to reversing dunes (Zimbelman, 2010).

3. Methodology

The DGPS surveys were carried out across the southernmost reversing dune at the Bruneau Dunes (Fig. 1). This location was chosen for the study because this dune progresses steadily from a low sand ridge into a large reversing dune (going north),

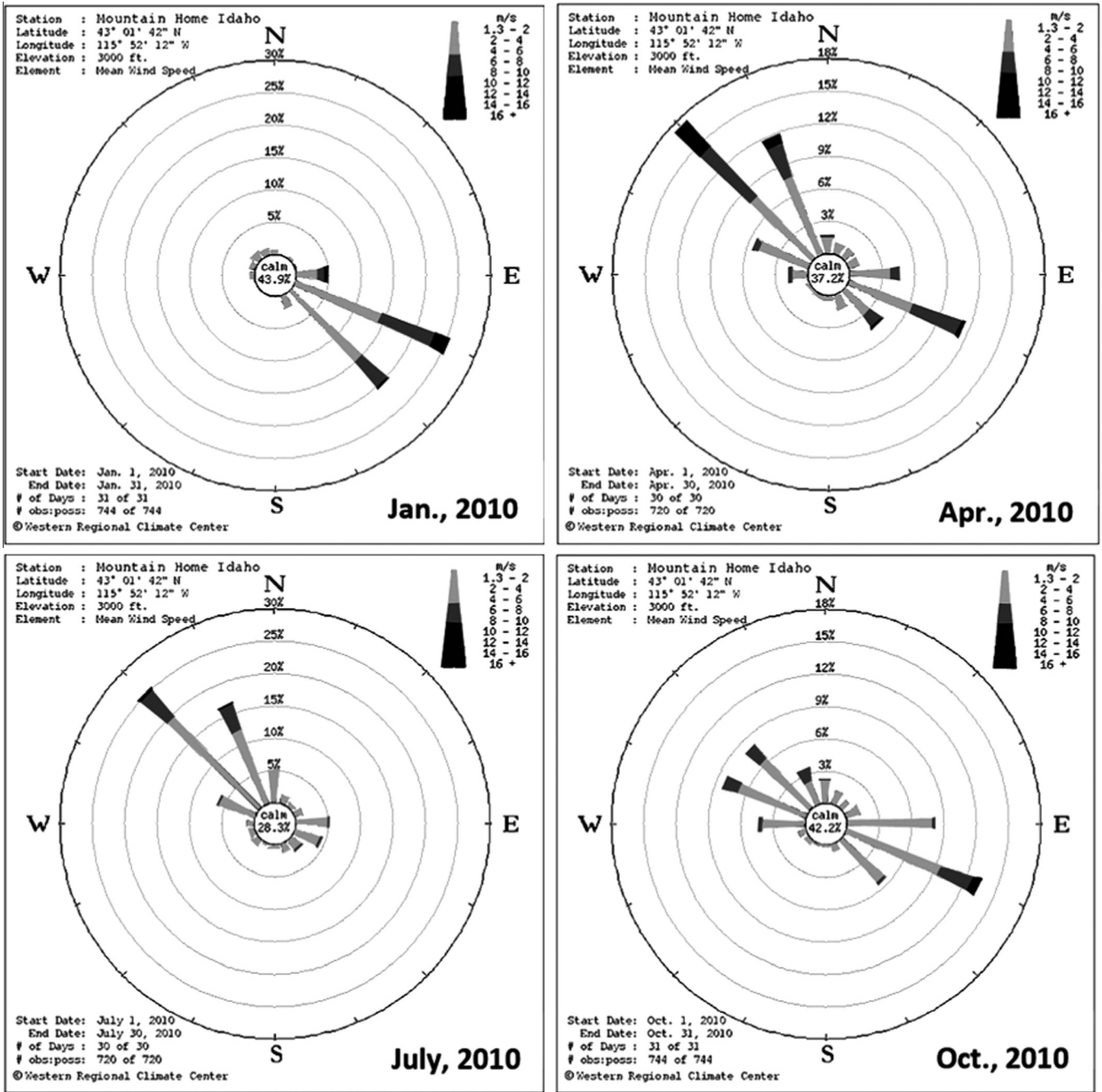


Fig. 2. Wind roses derived from RAWs data (Zachariassen et al., 2003) from station at the Mountain Home Air Force Base, located ~21 km NW of the Bruneau Dunes. Diagrams show the average wind strength and azimuth in four monthly averages during 2010. A seasonal bimodal wind pattern is evident, with spring and fall being transitional between oppositely directed winter and summer winds. Wind strength scale is simplified to three shades of gray; the two darkest gray shades are winds above the saltation threshold.

providing the opportunity to document the cross-sectional topography as it varies across the dune crest at a single site. The study location is well removed from the parking areas within the state park, which minimizes the public foot traffic at this part of the dune field, and thus maximizes the potential to document undisturbed dune morphology. Approximately a 1 h hike is required to go from a vehicle parking area (N42°54'2", W115°41'40"; WGS84) to the study site (N42°52'50", W115°41'57") by traversing around the east side of the main dunes. The northern tip of the Bruneau Dunes extends into a lake present near the parking areas (Fig. 1, inset), which would have required the surveys to end at the waterline rather than extend onto the surrounding terrain.

Intermediate portions of the Bruneau Dunes display substantial interactions between two main lines of reversing dunes, which would have complicated distinguishing the attributes of a single reversing dune at these locations.

On April 27, 2011, the authors conducted a series of ten DGPS traverses across the southern dune (Fig. 5). Traverse directions alternated between going W to E and going E to W as the surveys progressed upward in height along the dune crest. Labels in Fig. 5 indicate the start of each survey line. However, all topographic profiles presented below have been adjusted to represent distance across the dune beginning at the west side. The surveyed dune has a broad arcuate shape (Fig. 1), possibly influenced by some



Fig. 3. GardenWatchCam image of the southern end of the Bruneau Dunes showing strong saltation caused by wind from the NW (5/9/11).



Fig. 4. GardenWatchCam image of the southern end of the Bruneau Dunes showing strong saltation caused by wind from the SE (1/2/12).

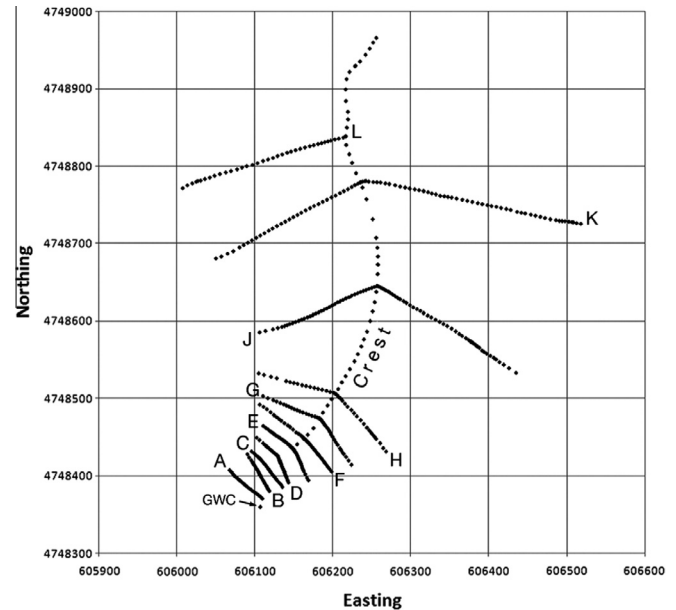


Fig. 5. Differential Global Positioning System (DGPS) transects across the southern end of the Bruneau Dunes, shown in UTM coordinates (Zone 11N). Profiles are labeled near the end of each line where that transect started. 'Crest' indicates points surveyed along the sharp crest after completing the profile transects. 'GWC' indicates the location of GardenWatchCam, looking NNE toward the summit of the southernmost large dune.

Table 1

Average slopes for the Bruneau reversing dune determined from DGPS surveys.

Profile	Slope (°) removed	h (m)	h/x W side	Slope (°)	h/x E side	Slope (°)
A	3.4W	1.0	0.0895	5.1	0.0342	2.0
B	3.3W	3.3	0.2157	12.2	0.1224	7.0
C	4.1W	4.7	0.2260	12.7	0.2185	12.3
D	4.2W	8.0	0.3627	19.9	0.3269	18.1
E	3.4W	13.1	0.3817	20.9	0.3098	17.2
F	3.2W	16.3	0.3286	18.2	0.3683	20.2
G	3.4W	24.7	0.4970	26.4	0.4495	24.2
H	2.3W	34.8	0.4184	22.7	0.4439	23.9
J	1.7W	76.1	0.5614	29.3	0.4158	22.6
K	1.4W	106.6	0.5602	29.3	0.3938	21.5
L	0	122.2	0.5478	28.7	–	–

subtle local topography revealed during the DGPS surveys. For traverses D to K, the survey line orientation was adjusted at the dune crest so that the line always followed the local path of maximum increase or decrease in height, which was perpendicular to the crest orientation encountered along each line. During each survey, one person operated the R8 roving receiver while the other person took notes and photographs keyed to the number assigned to each point along the survey line.

Ten survey lines (labeled A to K, skipping I) were collected across the dune, after which points were collected following the sharp crest going north along the dune. After completion of the crest survey, transect L was obtained going down the west side of the dune, starting at the highest point on the dune; this survey line passed close to an abandoned fence line, so a few of the fence posts were surveyed as possible control points for future DGPS surveys in this area. Surveys A through J were carried out using real time kinematic (RTK) DGPS where the rover and base stations had a clear line of sight between them. Surveys K through L and the crest survey were conducted using post processing kinematic (PPK) DGPS techniques using the same base station location as that of the RTK surveys. The accuracy of the individual DGPS positions

(<4 cm horizontal and vertical) means that differences between two surveyed points will be accurate to better than a decimeter, so relative distances and elevations reported here are listed to the nearest 0.1 m. Individual transect points were processed into profiles by calculating the distance between two adjacent points, then associating surveyed elevations to each point along the distance-based profile line. After a raw profile was generated, the local underlying slope could be determined, assisted by field notes that documented the points corresponding to the base of the dune. The local slope, determined by assuming a straight line between the base points on both sides of the dune (listed in Table 1), was then subtracted from each profile. Because profile L only covers the western side of the dune, no local slope was removed from it.

A GardenWatchCam timelapse digital camera was mounted 1.5 m above the sand surface on a post near the southern end of the surveyed dune ('GWC' in Fig. 5, which corresponds to the GPS location given above for the survey site) during the same trip used to collect the DGPS data. This camera has recorded hourly images of the surveyed dune that have documented major sand-driving events (e.g., Figs. 3 and 4) at the site since the surveys were

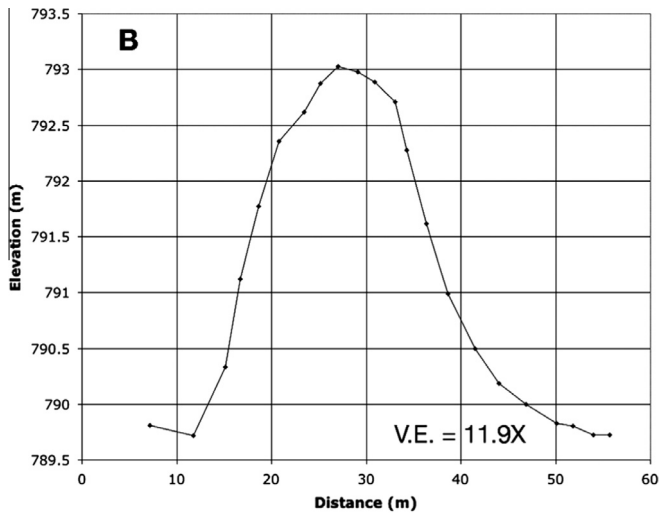


Fig. 6. DGPS survey B, showing a profile across an immature low sand ridge. Profile is shown going W to E, and a 3.3° West-dipping slope has been removed. Vertical exaggeration is 11.9 \times .

conducted, starting on April 27, 2011. More than 2 years of time-lapse image data (through August 31, 2013) have shown a close correlation between sand-driving events at the study site and strong winds recorded at the MHAFB RAWS station. It is beyond the scope of the present project to explore the RAWS wind records in depth, but the GardenWatchCam data increase our confidence that RAWS data from the MHAFB station are representative of the major wind activity experienced at the Bruneau Dunes.

4. Results

The DGPS data provide an interesting series of profiles that document how the topography of the reversing dune changes with distance up the axis of the dune. Local slopes removed from the profiles indicate that this portion of the dune has been built upon a shallow westward dipping slope (Table 1). Also, the surveyed elevations at the western base of the dune decrease by a cumulative 24.6 m going north from profiles A to L. The underlying local slopes and the decreasing elevations to the north suggest that the southern end of the dune likely lies across the southern margin of the shallow depression represented by Eagle Cove, with the lakes at the northern end of the dunes likely corresponding to the lowest part of the depression. It is at least possible that the subtle relief of the underlying depression may have contributed to the broad arcuate shape of the southern end of the dune (Fig. 1).

Profiles A to C cross the southern tip of the dune, where all three profiles are distinguished by low overall relief and the lack of a slip face; this part of the dune is essentially a low sand ridge. Profile B (Fig. 6) is typical of this immature section of the dune, the long axis of which is aligned with the axis of the main dune crest. During the collection of all three of these profiles, no field evidence was observed to indicate that flow separation was taking place as the sand moved over the sand ridge. However, following a few very strong wind events, a transient small (<15 cm high) sharp crest was visible in some GardenWatchCam images for the portion of the dune covered by profiles A to C, but such a feature rarely remained visible longer than a few days. Bagnold (1941, p. 183) observed in his wind tunnel that fully developed saltation induces a drag on the wind profile that resulted in sand deposition ~6 m downwind from where the intense saltation began; he inferred that this distance represented the minimum size of a dune, because over a distance smaller than this size sand is preferentially removed, whereas a

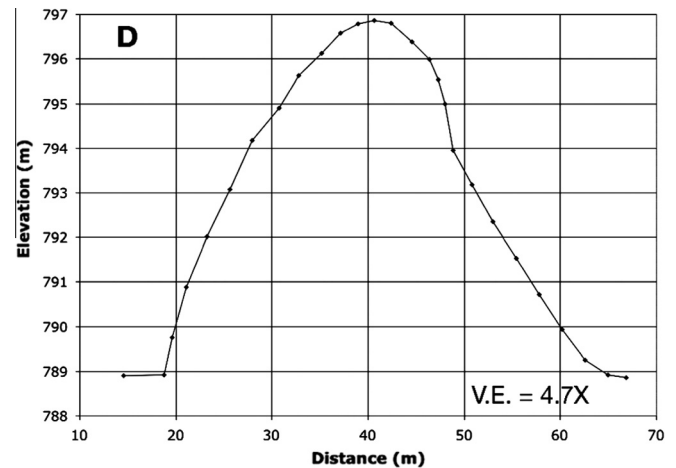


Fig. 7. DGPS survey D, showing a profile across a transitional part of the dune. Note subtle break in slope at ~48 m distance. Profile is shown going W to E, and a 4.2° West-dipping slope has been removed. Vertical exaggeration is 4.7 \times .

sand patch larger than this size will tend to grow through deposition. Today numerical models can investigate the physics of grain motions in the air and grain-to-grain interactions, so that a continuum saltation model provides the theoretical basis behind the minimum size of a sand dune (e.g., Sauermann et al., 2001). The three profiles across the immature sand ridge portion of the dune are ≥ 40 m in width, well in excess of Bagnold's minimum dune size. The presence or absence of a slip face should not be the defining characteristic for deciding whether or not a sand deposit can be considered to be a 'dune'.

Starting with profile D (Fig. 7), the sand ridge begins a transition toward the development of a sharp crest. While still lacking even a small slip face, profile D reveals that the top of the sand ridge has a broad pile of sand superposed on the smooth slope that typifies both of the lower flanks of the ridge (note the inflection point at ~48 m distance in Fig. 7). This feature is far too subtle to be readily apparent from visual inspection alone; a precision topographic transect was required to identify its presence. This low mound of sand at the top of the sand ridge may be better situated to respond to the alternating wind directions resulting from the bimodal wind regime associated with reversing dunes (e.g., Fig. 2), than would be the sand ridge itself.

The mound on top of the sand ridge finally has a small but distinct crest in profile E (Fig. 8). An inflection point similar to the one in profile D (Fig. 7) is present at ~53 m distance in profile E, but here the magnitude of the change in slope at the inflection point is considerably greater than the inflection point lower on the dune. Inflection points on the E side of both profiles D and E suggest that the most recent strong wind was from the west, consistent with the RAWS data for the weeks immediately preceding the survey work. Profile F has a good sharp crest, but it does not have an inflection point like the ones in profiles D and E, nor is the magnitude of its average flank slopes (Table 1) quite as large as those of a mature reversing dune, discussed next, so it appears to be transitional between mound-topped and mature profiles.

Profile G (Fig. 9) is the first profile that illustrates the main attribute of a mature reversing dune. Both sides of profile G are remarkably constant in slope away from the very sharp crest, giving a strong sense of symmetry to the profile. The average slope angle exceeds 24° on both sides of profile G (Table 1), but the average slope value ranges from 22° to 29° for the other mature profiles. As steep as these slope values are, they are still well below the angle of repose, which is the maximum angle (measured from horizontal) at which loose, cohesionless material will come to rest on

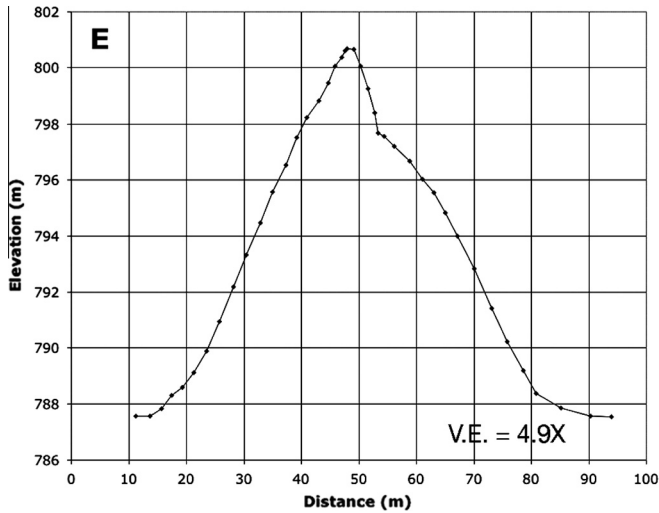


Fig. 8. DGPS survey E, showing a profile across a transitional part of the dune, with a mound present on top of a sand ridge base. Profile is shown going W to E, and a 3.4° West-dipping slope has been removed. Vertical exaggeration is $4.9\times$.

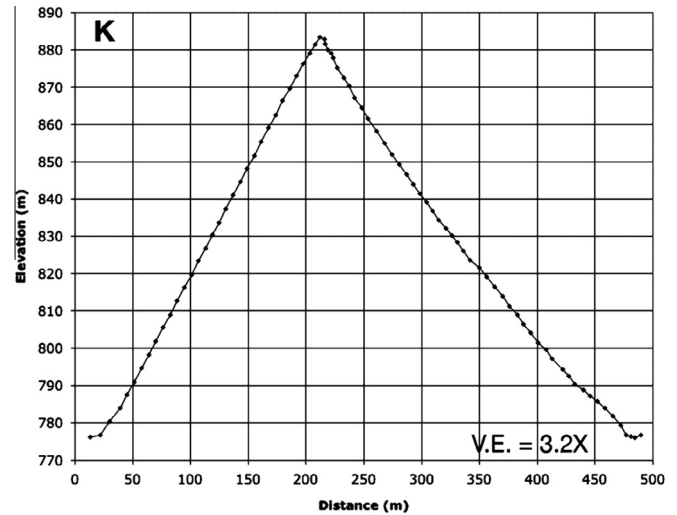


Fig. 10. DGPS survey K, showing a profile across a mature symmetric part of the dune, with 106.6 m of total relief. Profile is shown going W to E, and a 1.4° West-dipping slope has been removed. Vertical exaggeration is $3.2\times$.

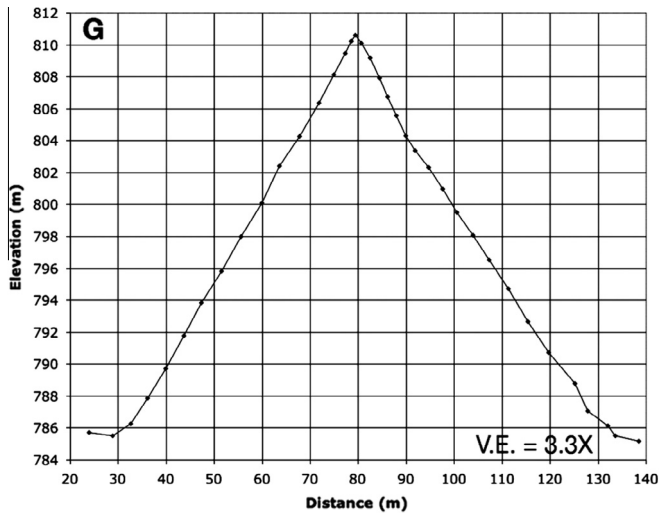


Fig. 9. DGPS survey G, showing a profile across a mature symmetric part of the dune, with 24.7 m of total relief. Profile is shown going W to E, and a 3.4° West-dipping slope has been removed. Vertical exaggeration $3.3\times$.

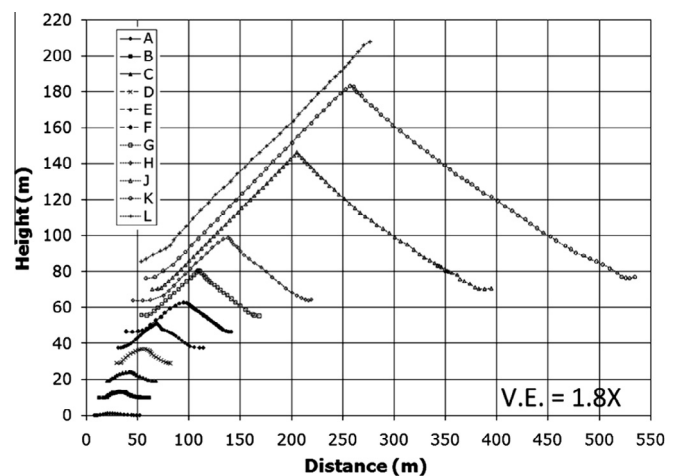


Fig. 11. All DGPS profiles at the Bruneau reversing dune, shown at the same scale. Successive profile starting points are offset 5 m horizontally and 10 m vertically, for clarity. Vertical exaggeration is $1.8\times$.

a pile of similar material (Jackson, 1997, p. 25). The angle of repose reported in the literature for dry sand on dune slip faces varies little from $33 \pm 1^\circ$ (Cooke and Warren, 1973, p. 276). Hence, the slopes of reversing dunes are not really very close to the slope found on a slip face, which is not surprising since sand will be moving back and forth across the dune crest, and thus cannot be near the angle of repose on both flanks at the same time. The sense of symmetry continues through profile K (Fig. 10) even as the total height and total width of the dune has steadily increased by more than a factor of four from profile G to K (Table 1). While not a complete profile, transect L documents that this reversing dune attains a maximum height of 122.2 m (Table 1).

It is difficult to appreciate the large change in scale that takes place across the surveyed profiles. When shown at the same horizontal and vertical scales (Fig. 11), the very low relief of the immature sand ridge profiles makes them almost indiscernible, although the large size of the mature profiles is readily apparent. Previous work has demonstrated that scaling both the horizontal and vertical dimensions by the feature width (defined as the distance

between the basal breaks in slope on both sides of the feature) is an effective way to preserve profile detail while comparing features that may differ by more than three orders of magnitude in absolute scale (Zimbelman et al., 2012). Fig. 12 shows the ten complete profiles for the Bruneau reversing dune when they have been scaled by the feature width (listed for each profile inside parentheses in the symbol key). Symbols and line styles help to distinguish between the three classes of profiles discussed above: immature sand ridge profiles in solid symbols and solid lines, transitional profiles in large dashed lines, and mature profiles in open symbols and small dashed lines. Along with preserving shape detail for each profile, this representation shows the steady increase in the scaled height for each profile; maximum height divided by feature width is therefore a key parameter for determining where along the ‘maturity’ continuum any single profile may lie, aided by details of the profile shape. It is particularly interesting to see how similar the four mature profiles appear, particularly on their west (left) side, which is consistent with the west being the windward side for the most recent strong winds. There is considerable variation in where the dune high point occurs along the scaled distance axis,

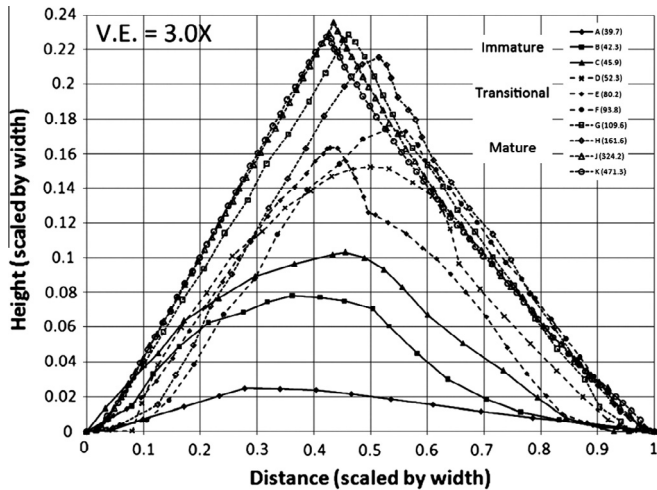


Fig. 12. Ten complete DGPS profiles from the Bruneau reversing dune, with both horizontal and vertical values scaled by the feature width for each profile (width values in m are listed in parentheses). Vertical exaggeration is 3.0×.

most likely due to local intensification or weakening of winds blowing over a feature as large as the Bruneau Dunes. Profiles in a composite width-scaled figure like Fig. 12 can serve as a general template to assess the relative maturity of features that are suspected of being reversing sand dunes, as discussed below.

The widely spaced points that followed the sharp crest line (Fig. 5) were sufficient to show a monotonic increase in elevation going up the dune, all the way to the local high point on transect L. From this local high, the elevation of the crest was broadly undulatory, gradually increasing 7.8 m in height while traversing 152 m north of transect L, so overall height of the biggest dunes slowly increases going north. At the same time, the topography on which the dunes are emplaced decreases toward the center of Eagle Cove, leading to the tallest dune (adjacent to the large lake) having a reported relief of 143 m. The surveyed DGPS points were imported into Google Earth following the conclusion of the field work, where we noted that the surveyed crest points did not correspond to the crest locations visible in the Google Earth images. Although the offset between some of the survey points and commercial images may be a result of a mismatch between coordinate systems or image geolocation accuracy, some parts of the survey lines matched up well with the image data. It is equally as likely that the crest location shifted in horizontal position between the times of image collection and the DGPS survey, raising the possibility that precise monitoring of crest location throughout the year may serve as a proxy for annual adjustments caused by fluctuations in seasonal wind patterns.

5. Discussion

The motivation for obtaining the topographic profiles at the Bruneau Dunes was to make use of the field data in evaluating the probable origins for TARs on Mars. HiRISE images finally show TARs with sufficient detail (Fig. 13) to make inferences about their shape from the way that the pixel brightness varies across an individual TAR. Three TAR profiles, corresponding to profiles A, C, and D of Zimbelman (2010), were scaled by their basal width to facilitate their direct comparison with three Bruneau profiles representing immature, transitional, and mature states of a reversing dune (Fig. 14). Two of the TAR profiles are most consistent with the transitional profile in terms of scaled height, although the martian features have much sharper crests than does the transitional profile. One TAR compares quite well with a mature profile from Bruneau,

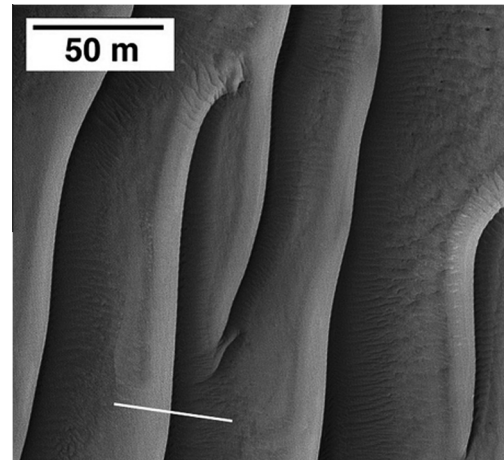


Fig. 13. Transverse Aeolian Ridges (TARs) on Mars. White line shows location of one profile (45.3 m width) that is included in Fig. 14. Portion of HiRISE image TRA_000823_1720, 7.7 S, 279.5 E, 25 cm/pixel. NASA/JPL-Caltech/U of A.

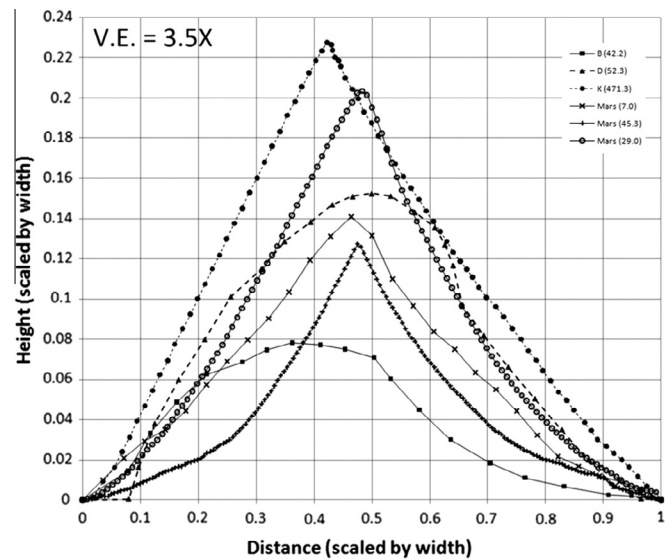


Fig. 14. Profiles of three Bruneau Dunes DGPS transects (closed symbols, profiles B, D, and K, this work) and three Mars TAR features (profiles A, C, and D, from Table 1 of Zimbelman (2010)), all scaled by feature width (width values in m are listed in parentheses). TARs are most similar to transitional and mature Bruneau profiles. Vertical exaggeration is 3.5×.

both in terms of profile shape and in maximum scaled height. Both profile shape and scaled height therefore suggest that TARs are generally more evolved than that of an immature sand ridge. Indeed, the overall shape of the sand ridge section of the Bruneau Dune (Fig. 6) is very similar to a profile across a broad sand patch on Mars (Fig. 6 of Zimbelman (2010)), consistent with the lack of either a sharp crest or a slip face visible on the martian sand patch. We interpret all of the above to suggest that large TARs (those larger than 1 m in height) are most similar to the transitional to mature parts of a growing reversing dune. This conclusion is also supported by observations that the topography across reversing dunes is measurably distinct from that of other transverse dunes, as well as from the topography across ripples, megaripples, and draa (Zimbelman et al., 2012). However, it is important to note that reversing dunes form under rather specific wind conditions, wind patterns that may be difficult to reconcile with the nearly planet-wide distribution of TARs on Mars (e.g., Balme et al., 2008; Berman et al., 2011).

The high degree of symmetry of most TAR profiles (Shockey and Zimbelman, 2013) argues strongly that bimodal winds of comparable strength and intensity may have been involved in their formation. Dramatic temperature extremes are generated globally on Mars by the thin martian atmosphere, whose relatively small heat capacity means that it cools and heats much more rapidly than our own atmosphere throughout the course of a day (Carr, 1981, p. 27). Possibly the dramatic diurnal temperature extremes on Mars may cause strong tidal winds, particularly where those winds become channeled within a valley or between broad topographic highs. Still, it is difficult to reconcile the wide distribution of TARs across Mars with the global wind patterns that exist at present (e.g., Zurek et al., 1992). The annual bimodal winds typical of the Bruneau area (Fig. 2) might be more similar to seasonal changes in wind patterns on Mars, but such relationships need to be explored by meteorological investigations well beyond the scope of the present study.

Maximum height scaled by width appears to be an important topographic parameter for evaluating the likely origin of aeolian bedforms (Zimbelman et al., 2012). Fig. 15 compares height/width values as a function of width for measured profiles from dozens of megaripples and transverse dunes on Earth (data from Fig. 5 of Zimbelman et al. (2012)) to values derived from the ten Bruneau profiles (large filled circles), and also to more than seventy TARs on Mars (small dots; data from Zimbelman (2010), and Shockey and Zimbelman (2013)). Several interesting trends are apparent from all of these data; we will first examine the track followed by points derived from the ten Bruneau profiles.

For the immature sand ridge section of the Bruneau reversing dune, values of height/width increase steadily as the profiles progress up the dune while overall width remains nearly constant. In general, height/width <0.13 appears to represent the immature phase of reversing dune development, where vertical growth entirely dominates over any significant increase in the width of the feature. The transitional phase of the Bruneau profiles begins at a point consistent with the trend followed in the immature section, but now the height/width values increase from 0.15 to 0.18 while at the same time width more than doubles. Vertical growth continues in this section, but now dune width also grows at roughly half the rate as the growing height. Once the mature stage is reached,

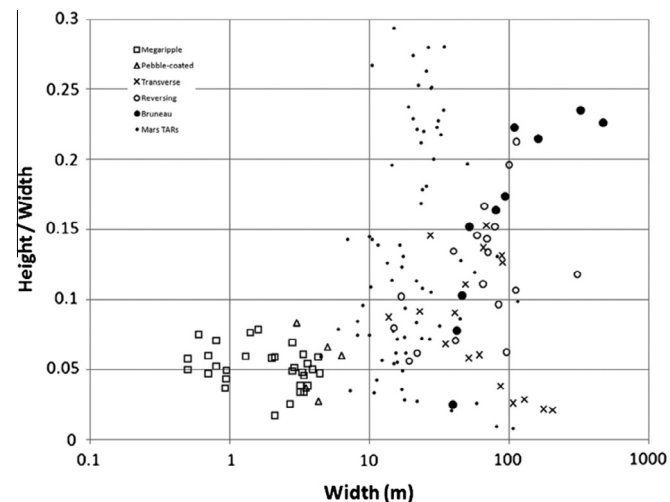


Fig. 15. Height/width as a function of log width, for features on Earth and Mars. Megaripple (open squares), pebble-coated megaripple (open triangle), transverse dune (x's), and reversing dunes (open circles) data are from the supplementary data file of Zimbelman et al. (2012). Bruneau reversing dune data (large filled circles) are from this work. Mars TAR data (small dots) are from Table 1 of Zimbelman (2010) and the supplementary data file of Shockey and Zimbelman (2013). See Section 5 of text.

height/width remains between 0.21 and 0.24 while height and width now change in lock step; height/width changes relatively little while width increases by more than a factor of five. Only reversing dunes (open and closed circles in Fig. 15) experience vertical growth sufficient to raise their height/width values well above ~ 0.15 , which is the maximum value attained by transverse dunes (\times in Fig. 15).

The overall trend outlined above is consistent with measurements that are less precise than what is obtained through DGPS; the two largest height/width values previously reported for reversing dunes also come from the Bruneau Dunes, where a less precise laser inclinometer (precision of individual measurements was 0.3 m) produced values that fall along the trend between the transitional and mature DGPS points. Physical dimensions of dune-like features obtained from laboratory or numerical studies (e.g., Reffet et al., 2010; Taniguchi et al., 2012) should be amenable to comparison with the measured attributes shown in Fig. 15. Kocurek et al. (1992) documented the seasonal construction and destruction of sand dunes on Padre Island, Texas, with dunes growing from small patches of sand into regular dunes, which were subsequently removed by winter storm winds, a situation that may warrant comparison to the Bruneau Dunes. We believe that the DGPS data from Bruneau reveal an evolutionary path that can be followed in a plot of height/width as a function of width, a path that might be explored through comparison with reversing dunes developed in a variety of formational settings.

Next consider the cloud of data points that represent measurements from dozens of TARs (small dots in Fig. 15) from locations scattered across Mars. The Mars TAR data come from measured heights and widths given in Table 1 of Zimbelman (2010; 13 TARs) and in the supplementary data file of Shockey and Zimbelman (2013; 60 TARs). In Fig. 15, the TAR data fill a gap between the fields representing values for megaripples (open squares) and pebble-coated megaripples (open triangles) and the values for transverse (\times s) and reversing (open circles) dunes. The height-width distribution of TARs is generally similar to that of reversing dunes, but the measured height/width values of TARs extend to as much as twice that of transverse dunes, but are similar in shape to the overall trend for reversing dunes. While some of the TAR data points do overlap with the immature portion of the Bruneau trend, we do not believe this superposition indicates that most TARs are good matches to the immature part of the Bruneau reversing dune, particularly when the sharp-peaked symmetric profile shape for TARs (Fig. 14) is considered. Instead, the similarity of the overall range of height/width values between TARs and reversing dunes, but at widths scales generally 1/3 that of reversing dunes on Earth, raises the intriguing possibility that the reduced gravity of Mars (38% that on Earth) somehow contributes to the development of smaller symmetric TAR features on Mars relative to comparable features on Earth. We are unaware of a physical explanation for how the lower gravity on Mars should somehow result in martian landforms smaller than terrestrial counterparts, particularly since the low gravity and low atmospheric pressure cause sand saltation path lengths to be >10 times longer on Mars than they are on Earth (White, 1979). It is unwise to speculate too extensively on what is still a relatively limited data set derived from cross-sectional profiles for the features on both Earth and Mars, but these initial comparisons suggest that the height/width as a function of width parameter space warrants further investigation for features on both planets.

The height/width values in excess of 0.25 come from TARs at relatively high latitudes (lat. >30°N or S on Mars). It seems possible that features at mid- to high latitudes may include ground ice that would facilitate vertical growth beyond that of unconsolidated sand alone (a pile of sand with a slope angle of 33° would have a height/width value of 0.325). Another possibility is that during

long periods of stability (~50–200 ka inactivity for megaripples in Meridiani Planum, Golombek et al., 2010), dust that settled out of the atmosphere may filter between the particles on TARs and increase the angle of internal friction beyond that of unconsolidated materials alone, although if this effect is significant, it should occur anywhere on Mars rather than preferentially at high latitudes. Long periods of stability for megaripples (and TARs) on Mars would mean that wind patterns inferred from such features could be related to winds generated by conditions quite different from the present state of the atmosphere.

6. Summary

Ten precision profiles of a reversing dune show a progression from immature (lacking a sharp crest or slip face) sand ridge to mature (symmetric) reversing dune, for which both slopes are near the angle of repose. When scaled by the basal width of the feature, the Bruneau profiles can be compared to profiles of Transverse Aeolian Ridges (TARs) on Mars; this comparison suggests that many TARs are similar to either transitional or mature reversing dune profiles.

Acknowledgments

Comments by two anonymous reviewers were very helpful during revision of the manuscript. This research was supported by funds from the Becker portion of the Smithsonian Endowments.

References

- Bagnold, R.A., 1941. *The Physics of Blown Sand and Desert Dunes*. Chapman and Hall, London, UK, 265p.
- Balme, M., Berman, D.C., Bourke, M.C., Zimbelman, J.R., 2008. Transverse aeolian ridges (TARs) on Mars. *Geomorphology* 101, 703–720.
- Berman, D.C., Balme, M.R., Rafkin, S.C.R., Zimbelman, J.R., 2011. Transverse aeolian ridges (TARs) on Mars II: distributions, orientations, and ages. *Icarus* 213, 116–130.
- Bourke, M.C., Wilson, S.A., Zimbelman, J.R., 2003. The variability of Transverse Aeolian Ridges in troughs on Mars. *Lunar Planet. Sci.* XXXIV, Abstract #2090.
- Carr, M.H., 1981. *The Surface of Mars*. Yale Univ. Pr., New Haven, 232p.
- Cooke, R.U., Warren, A., 1973. *Geomorphology in Deserts*. Univ. Calif. Pr., Berkeley, CA, 394p.
- Golombek, M. et al., 2010. Constraints on ripple migration at Meridiani Planum from Opportunity and HiRISE observations of fresh craters. *J. Geophys. Res.* 115, E00F08. <http://dx.doi.org/10.1029/2010JE003628>.
- Howard, A.D., Morton, J.B., Gad-el-Hak, M., Pierce, D., 1978. Sand transport model of barchan dune evolution. *Sedimentology* 25, 307–338.
- Irwin, R.P., Zimbelman, J.R., 2012. Morphometry of Great Basin pluvial shore landforms: Implications for paleolake basins on Mars. *J. Geophys. Res.* 117, E07004. <http://dx.doi.org/10.1029/2012JE004046>.
- Jackson, J.A. (Ed.), 1997. *Glossary of Geology*, fourth ed. Am. Geol. Inst., Alexandria, pp. 769.
- Jarrett, R.D., Malde, H.E., 1987. Paleodischarge of the late Pleistocene Bonneville Flood, Snake River, Idaho, computed from new evidence. *Geol. Soc. Am. Bull.* 99, 127–134.
- Kocurek, G., Townsley, M., Yeh, E., Havholm, K.G., Sweet, M.L., 1992. Dune and dune-field development on Padre Island, Texas, with implications for interdune deposition and water-table-controlled accumulation. *J. Sed. Res.* 62 (4), 622–635.
- Lancaster, N., 1989. The dynamics of star dunes: An example from the Gran Desierto, Mexico. *Sedimentology* 36, 273–289.
- Lorenz, R.D., 2011. Observations of wind ripple migration on an Egyptian seif dune using an inexpensive digital timelapse camera. *Aeol. Res.* 3 (2), 229–234. <http://dx.doi.org/10.1016/j.aeolia.2011.01.004>.
- Lorenz, R.D., Valdez, A., 2011. Variable wind ripple migration at Great Sand Dunes National Park and Preserve, observed by timelapse imagery. *Geomorphology* 133 (1–2), 1–10. <http://dx.doi.org/10.1016/j.geomorph.2011.06.003>.
- Malde, H.E., 1968. The catastrophic late Pleistocene Bonneville Flood in the Snake River Plain, Idaho. U.S. Geol. Surv. Prof. Paper 596. 52p.
- McEwen, A.S. et al., 2007. Mars Reconnaissance Orbiter's High Resolution Imaging Science Experiment (HiRISE). *J. Geophys. Res.* 112, E05S02. <http://dx.doi.org/10.1029/2005JE002605>.
- McKee, E.D., 1979. Introduction to a study of global sand seas. In: McKee, E.D. (Ed.), *A Study of Global Sand Seas*. U.S. Geol. Surv. Prof. Paper 1052. Gov. Printing Office, Washington, DC, pp. 1–19.
- Murphy, J.D., 1973. The Geology of Eagle Cove at Bruneau, Idaho. M.S. Thesis, State Univ. New York at Buffalo. 77p.
- O'Connor, J.E., 1993. Hydrology, Hydraulics, and Geomorphology of the Bonneville Flood. *Geol. Soc. Am. Sp. Paper* 274. 83p.
- Reffet, E., du Pont, S.C., Hersen, P., Douady, S., 2010. Formation and stability of transverse and longitudinal sand dunes. *Geology* 38 (6), 491–494. <http://dx.doi.org/10.1130/G30894.1>.
- Sauermann, G., Kroy, K., Hermann, H.J., 2001. Continuum saltation model for sand dunes. *Phys. Rev. E* 64, 031305. <http://dx.doi.org/10.1103/PhysRevE.64.031305>.
- Shockey, K.M., Zimbelman, J.R., 2013. Analysis of transverse aeolian ridge profiles derived from HiRISE images of Mars. *Earth Surf. Process. Landforms* 38, 179–182. <http://dx.doi.org/10.1002/esp.3316>.
- Taniguchi, K., Endo, N., Sekiguchi, H., 2012. The effect of periodic changes in wind direction on the deformation and morphology of isolated sand dunes based on flume experiments and field data from the Western Sahara. *Geomorphology* 179, 286–299. <http://dx.doi.org/10.1016/j.geomorph.2012.08.019>.
- White, B.R., 1979. Soil transport by winds on Mars. *J. Geophys. Res.* 84, 4644–4651.
- Zachariassen, J., Zeller, K., Nikolov, N., McClelland, T., 2003. A Review of the Forest Service Remote Automated Weather Station (RAWS) Network. Gen. Tech. Rpt RMRS-GTR-119. U.S. Dept. Agric. and Forest Serv., Ft. Collins, CO. 163p.
- Zimbelman, J.R., 2010. Transverse Aeolian Ridges on Mars: First results from HiRISE images. *Geomorphology* 121, 22–29. <http://dx.doi.org/10.1016/j.geomorph.2009.05.012>.
- Zimbelman, J.R., Johnston, A.K., 2001. Improved topography of the Carrizozo lava flow: Implications for emplacement conditions. In: Crumpler, L.S., Lucas, S.G. (Eds.), *Volcanology in New Mexico*. New Mex. Mus. Nat. Hist. Sci. Bull. 178, Albuquerque, NM, pp. 131–136.
- Zimbelman, J.R., Scheidt, S.P., 2012. Topographic profiles across a large reversing dune, to aid in evaluating the reversing dune hypothesis for TARs on Mars. In: Third International Planetary Dunes Workshop: Remote Sensing and Data Analysis of Planetary Dunes, LPI Contribution 1673, Lunar and Planetary Institute, Houston, pp. 105–106.
- Zimbelman, J.R., Williams, S.H., 2007. Eolian dunes and deposits in the western United States as analogs to wind-related features on Mars. In: Chapman, M.G. (Ed.), *The Geology of Mars: Evidence from Earth-based Analogs*. Cambridge Univ. Pr., Cambridge, UK, pp. 232–264.
- Zimbelman, J.R., Williams, S.H., Johnston, A.K., 2012. Cross-sectional profiles of sand ripples, megaripples, and dunes: A method for discriminating between formational mechanisms. *Earth Surf. Process. Landforms* 37, 1120–1125. <http://dx.doi.org/10.1002/esp.3243>.
- Zurek, R.W., Barnes, J.R., Haberle, R.M., Pollack, J.B., Tillman, J.E., Leovy, C.B., 1992. Dynamics of the atmosphere of Mars. In: Kieffer, H.H., Jakosky, B.M., Snyder, C.W., Matthews, M.S. (Eds.), *Mars. Univ. of Arizona Pr., Tucson*, pp. 835–933.